

# Partitioned-Matrix acceleration to the Fission-Source iteration of the Variational Nodal Method



Yunzhao Li <sup>a,\*</sup>, Yongping Wang <sup>a</sup>, Boning Liang <sup>a</sup>, Wei Shen <sup>a,b</sup>

<sup>a</sup> School of Nuclear Science and Technology, Xi'an Jiaotong University, China

<sup>b</sup> Canadian Nuclear Safety Commission, Canada

## ARTICLE INFO

### Article history:

Received 1 June 2015

Received in revised form

27 July 2015

Accepted 3 August 2015

Available online 3 September 2015

### Keywords:

Variational Nodal Method

Neutron-diffusion calculation

PWR

Partitioned-Matrix acceleration

Fission-Source iteration

## ABSTRACT

The Variational Nodal Method (VNM) expands the nodal volumetric flux and surface partial current into the sums of orthogonal basis functions without using the transverse integration technique. The exclusion of the transverse integration provides a number of advantages for employing the VNM in Pressurized Water Reactor (PWR) core simulation. The orthogonality of those basis functions guarantees the conservation of neutron balance regardless of the expansion orders, providing an opportunity to accelerate the computationally expensive full-order iteration by using cheap low-order sweeping with high-order moments fixed. This was named as the Partitioned-Matrix (PM) technique in the legacy VNM code VARIANT, and was applied to the within-group (WG) iteration. It is very effective for neutron-transport calculation, but less effective for neutron-diffusion mainly due to the reduced number of high-order partial current moments. In this paper, we extend the PM technique to the Fission-Source (FS) iteration to accelerate the flux convergence by using low-order flux moments also. From the macroscopic acceleration point of view, it converges the fission- and scattering-source distributions by using computationally cheap low-order iteration faster than the original full-order sweeping. Based on our new VNM code VIOLET, considering the fact that the discontinuity factor used for preserving neutron leakage rates during spatial homogenization slows down the nodal iteration convergence, numerical tests were carried out for two typical PWR problems respectively without and with discontinuity factors. By analyzing both the computational effort in terms of FLOP (Floating-point Operation) and computing time, the following conclusions have been demonstrated. The legacy PM technique for WG iteration can provide an acceleration ratio of about 2 for the PWR core neutron-diffusion calculation with or without using discontinuity factors, while the one for FS iteration itself can accelerate by a factor of about 3 which is higher. By accelerating both the WG and FS iteration simultaneously, the acceleration ratio is about 4 for both the two PWR problems. In addition, by extending the PM technique from the WG iteration to the FS iteration, the neutron-diffusion calculation of the VNM can be accelerated very effectively with almost no extra storage or implementation cost to the existing computer code.

© 2015 Elsevier Ltd. All rights reserved.

## 1. Introduction

The Variational Nodal Method (VNM) (Lewis and Miller, 1984; Carrico et al., 1992) was first developed by Northwestern University and Argonne National Laboratory (ANL) to solve the multi-group steady-state neutron-diffusion and -transport equations for reactor core calculations. It uses a variational principle for the even-

parity form of the Boltzmann transport equation. In this variational principle, the odd-parity Lagrange multipliers along the nodal interfaces guarantee neutron conservation for each node. The classical Ritz procedure is employed by using orthogonal polynomials in space and spherical harmonics in angle. Nodal response matrices are then formed for the volumetric flux moments and surface partial current moments. The VARIANT code (Palmiotti et al., 1995), developed at ANL in mid 90s was the first production code based on VNM. It has been employed for fast reactor routinely designing both in ANL such as the REBUS code (Toppel, March 1983) and in Europe such as the ERANOS code (Doriath et al., 1994). In 2007, a new version of the VARIANT code named NODAL was developed in ANL

\* Corresponding author. School of Nuclear Science and Technology, Xi'an Jiaotong University, 28 West Xianning Road, Xi'an, Shaanxi 710049, China.

E-mail address: [yunzhao@mail.xjtu.edu.cn](mailto:yunzhao@mail.xjtu.edu.cn) (Y. Li).

as one of the solvers in the UNIC package (Palmiotti et al., 2007; Li et al., 2015). In 2011, it has also been implemented into the INSTANT code in Idaho National Laboratory (INL) (Wang et al., 2011).

The exclusion of the transverse integration in the VNM provides several advantages (Lawrence, 1986; Wagner, 1989). Firstly, the VNM expands the volume flux by using basis functions which usually are orthogonal polynomials. Once obtained those flux moments, continuous flux profile within each node can be obtained, leaving no need for pin power reconstruction which usually introduces more approximations. Secondly, for adjoint flux calculation usually employed in transient simulation, the VNM can guarantee that the corresponding mathematical adjoint flux is exactly the same with the physical one. Thirdly, it is possible to extend the homogeneous VNM to heterogeneous VNM which can treat heterogeneous cross section distribution within each node (Smith et al., 2003; Li et al., 2014; Wang et al.). Fourthly, the VNM employs the Pn method for angular variable within which neutron-diffusion equation is equivalent to the P<sub>1</sub> approximation, enabling this method can to be consistently extended to neutron-transport calculation. Thus, recently a new VNM code named VIOLET has been developed at Xi'an Jiaotong University (XJTU) for thermal reactor such as Pressurized Water Reactor (PWR) neutron-diffusion simulation.

The numerical process of the VNM contains three levels of iteration. The outermost is the Fission-Source (FS) iteration (also termed as the outer iteration in literatures) based upon the Power Method (Lewis and Miller, 1984). At each FS iteration, just in case if up-scattering shows up, the multi-group (MG) flux system is solved by using the legacy Gauss-Seidel (GS) algorithm. Only one sweep over the energy groups is required if there is no up-scattering. For each group, the within-group (WG) response matrix system is solved by using the Red-Black Gauss-Seidel (RBGS) algorithm (Palmiotti et al., 1995). It is the so-called WG iteration (typically termed as the inner iteration in literatures).

Traditionally, the VARIANT code employs the Partitioned-Matrix (PM) technique to accelerate the WG iteration. Before each full-order partial current moments iteration, a number of low-order partial current moments iterations are carried out with the high-order ones fixed. Usually, only one full-order sweep is carried out for each energy group within each MG iteration. The PM technique performs very well in transport cases due to the large number of high-order moments. However, the effect is less effective in diffusion because there are fewer high-order moments to eliminate. Though other techniques or algorithms such as the Krylov (Saad, 2003; Saad and Schultz, 1986) ones including CG (Conjugate Gradient) (Wang et al., 2011) and GMRES (Generalized Minimal Residual Method) (Wang et al., 2011; Lewis et al., 2013; Li et al., 2012) have also been proposed and tested, they usually require more memory due to the storage of orthogonal vectors. In addition, these algorithms usually require preconditioners to be compatible with the PM accelerated WG RBGS iteration, making the code system much more complicated.

The rest of this paper is organized as following. Section 2 describes the theory of the VNM including its iteration process, the PM technique and its implementations to the both the WG and FS iterations of the VNM, Section 3 assesses the PM technique numerically by using two typical PWR problems respectively with and without discontinuity factors. Section 4 summarizes the conclusions and discussions.

## 2. Theoretical formulation

After introducing the VNM response matrices and the iteration process, the PM techniques for both the WG and FS iterations are described in detail. The computing efforts of applying these

response matrices are evaluated and summarized based on these formulas.

### 2.1. The Variational Nodal Method

After the multi-group approximation for the energy variable and the P<sub>1</sub> approximation for the angular variable, isotropic scattering with transport correction and isotropic fission, the neutron-transport equation becomes the Multi-Group neutron-diffusion equation together with its albedo boundary condition:

$$\begin{cases} \nabla \mathbf{J}_g + \sum_{r,g} \Phi_g = S_g \\ \frac{1}{3} \nabla \Phi_g + \sum_{r,g} \mathbf{J}_g = 0 \end{cases}, g = 1 \sim G \quad (1)$$

$$S_g = \sum_{g' \neq g} \sum_{s,gg'} \Phi_{g'} + \frac{1}{k} \sum_{g'} F_{gg'} \Phi_{g'} \quad (2)$$

$$\Phi_g - 2\mathbf{J}_g^T \mathbf{n}_\gamma = \beta_{\gamma,g} \cdot (\Phi_g + 2\mathbf{J}_g^T \mathbf{n}_\gamma), \quad \mathbf{r} \in \Gamma_\gamma \quad (3)$$

where common symbols are used as in literature (Lewis and Miller, 1984),  $\mathbf{J}_g$  and  $\mathbf{n}_\gamma$  are column vectors. The variational principle (Lewis and Miller, 1984) turns out to be:

$$F[\Phi_g, \mathbf{J}_g] = \sum_\nu F_\nu[\Phi_g, \mathbf{J}_g] \quad (4)$$

$$\begin{aligned} F_\nu[\Phi_g, \mathbf{J}_g] = & \int_\nu dV \left\{ (3\Sigma_{tr,g})^{-1} \nabla \Phi_g \nabla \Phi_g + \Sigma_{r,g} \Phi_g^2 - 2\Phi_g S_g \right\} + 2 \\ & \times \sum_\gamma \int_\gamma \Phi_g \cdot \mathbf{J}_g^T \mathbf{n}_\gamma d\Gamma \end{aligned} \quad (5)$$

For each energy group and each node, the volumetric flux and source are expanded by using basis functions:

$$\Phi_g(\mathbf{r}) = \sum_{i=1}^I \phi_{i,g} f_i(\mathbf{r}) = \mathbf{f}^T \boldsymbol{\phi}_g, \quad \mathbf{r} \in \nu \quad (6)$$

$$S_g(\mathbf{r}) = \sum_{i=1}^I s_{i,g} f_i(\mathbf{r}) = \mathbf{f}^T \mathbf{s}_g, \quad \mathbf{r} \in \nu \quad (7)$$

And the surface net outgoing current is expanded as

$$\mathbf{J}_g^T(\mathbf{r}) \mathbf{n}_\gamma = \sum_{k=1}^K j_{\gamma,k,g} h_{\gamma,k}(\mathbf{r}) = \mathbf{h}_\gamma^T \mathbf{j}_{\gamma,g}, \quad \mathbf{r} \in \Gamma_\gamma \quad (8)$$

where  $f_i(\mathbf{r})$  and  $h_{\gamma,k}(\mathbf{r})$  are orthogonal polynomial basis functions respectively on nodal volume  $\nu$  and surface  $\Gamma_\gamma$ ,  $I$  and  $K$  are the number of expansion terms,  $\boldsymbol{\phi}_g$ ,  $\mathbf{s}_g$ ,  $\mathbf{j}_{\gamma,g}$ ,  $\mathbf{f}$  and  $\mathbf{h}_\gamma$  are column vectors containing the corresponding moments and functions.

Nodal response matrices can be formed (Lewis and Miller, 1984; Carrico et al., 1992; Palmiotti et al., 1995; Wang et al., 2011) by firstly substituting the expansions in Eqs. (6)–(8) into the functional in Eq. (5), the boundary conditions in Eq. (3) and the source in Eq. (2) and then requiring the functional to be stable in terms of  $\boldsymbol{\phi}_g$  and  $\mathbf{j}_g$  respectively:

$$\mathbf{s}_g = \sum_{g' \neq g} \Sigma_{gg'} \boldsymbol{\varphi}_{g'} + \frac{1}{k} \sum_{g'} F_{gg'} \boldsymbol{\varphi}_{g'} \quad (9)$$

$$\mathbf{j}_g^+ = \mathbf{R}_g \boldsymbol{\Pi} \otimes \mathbf{I}_K \mathbf{j}_g^+ + \mathbf{B}_g \mathbf{s}_g \quad (10)$$

$$\boldsymbol{\varphi}_g = \mathbf{H}_g \mathbf{s}_g - \mathbf{C}_g (\mathbf{I}_{N \cdot N_s} - \boldsymbol{\Pi}) \otimes \mathbf{I}_K \mathbf{j}_g^+ \quad (11)$$

where  $\boldsymbol{\Pi}$  stands for the spatial connection matrix containing the albedo outer boundary condition and the continuity inner boundary condition,  $\mathbf{I}_X$  stands for an  $X \times X$  identity matrix,  $N$  is the number of nodes,  $N_s$  is the number of surfaces per node,  $\otimes$  refers to tensor product between the two matrices, the surface partial current vector is defined as

$$\mathbf{j}_g^\pm = \frac{1}{4} \mathbf{M}^T \boldsymbol{\varphi}_g \pm \frac{1}{2} \mathbf{j}_g \quad (12)$$

$$\mathbf{j}_g = \left[ \mathbf{j}_{1,g}^T \quad \cdots \quad \mathbf{j}_{\gamma,g}^T \quad \cdots \right]^T \quad (13)$$

The response matrices  $\mathbf{R}$ ,  $\mathbf{B}$ ,  $\mathbf{H}$ ,  $\mathbf{C}$  and  $\mathbf{M}$ , depends on nodal geometry, material and the volumetric and surface expansion orders, are block diagonal over spatial nodes and can be found elsewhere (Palmiotti et al., 1995). Once the discontinuity factors (DF) show up, this inner boundary condition can be obtained by imposing net current continuity and flux discontinuity:

$$\mathbf{j}_{\gamma,g}^- = \frac{2f_{\gamma'}}{f_{\gamma'} + f_{\gamma}} \mathbf{j}_{\gamma',g}^+ + \frac{f_{\gamma'} - f_{\gamma}}{f_{\gamma'} + f_{\gamma}} \mathbf{j}_{\gamma,g}^+ \quad (14)$$

$f_{\gamma}$  and  $f_{\gamma'}$  are the discontinuity factors (DF) of the two adjacent nodes  $\gamma$  and  $\gamma'$  obtained by using the legacy Generalized Equivalence Theory (GET) (Smith, 1986, 1980).

The appearance of the fission source makes the above equation an eigenvalue problem. The legacy Power Method (Lewis and Miller, 1984; Xie and Deng, 2005) is employed and referred as Fission-Source (FS) iteration here. Within each FS iteration, the flux has to be updated with fission source fixed by employing the legacy Gauss-Seidel algorithm. This iteration is termed as multi-group (MG) iteration. It is noticeable that only one MG iteration would be required if there is no up-scattering which is usually the case for the PWR core diffusion calculation. Within each MG iteration, the flux vector is updated one group after another, which means there is an sweeping from the 1st energy group to the  $G$ 'th energy group. For each energy group, a) the source is constructed by using Eq. (9), b) the current is iteratively updated as in Eq. (10) by employing the Red-Black Gauss-Seidel (RBGS) algorithm, c) the flux is constructed by using the neutron balance equation in Eq. (11).

The iteration process of VNM is shown in Fig. 1. It has to be pointed out that there is an Absolute Error Tolerance (AET) and a Relative Error Tolerance (RET) used as the iterative vector convergence criteria. Taking vector  $\mathbf{v}$  as an example, the AET  $\varepsilon_v$  and RET  $e_v$  are as following:

$$r^{(i)} = \frac{\|\mathbf{v}^{(i)} - \mathbf{v}^{(i-1)}\|_2}{\|\mathbf{v}^{(i)}\|_2} \quad (15)$$

$$r^{(i)} < \varepsilon_v \quad (16)$$

$$\frac{r^{(i)}}{r^{(1)}} < e_v. \quad (17)$$

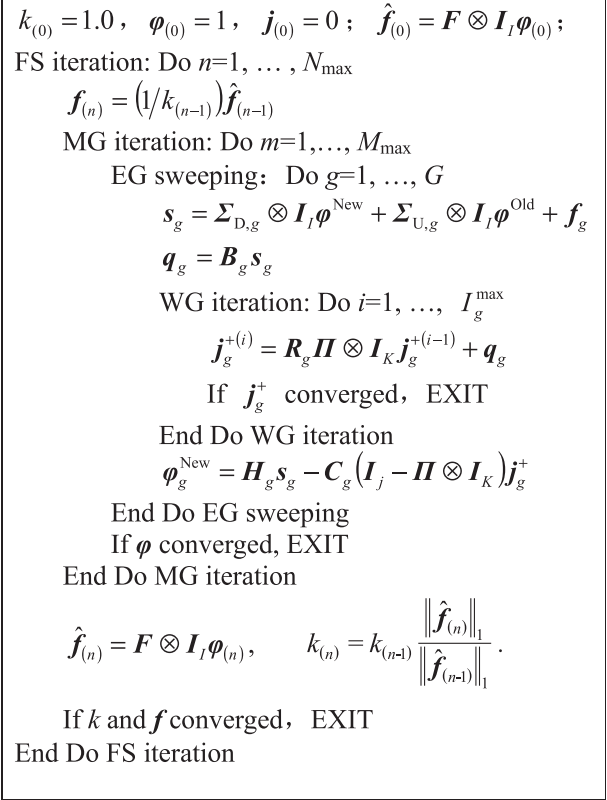


Fig. 1. The VNM iteration process.

## 2.2. The Partitioned-Matrix acceleration for within-group iteration

Because of the hierarchical system of orthogonal polynomials in space, a low-order system can closely resemble the original full-order system by maintaining neutron balance. Thus, traditionally the Partitioned-Matrix (PM) technique is applied to the within-group (WG) iteration.

Partitioning the surface partial current vector:

$$\mathbf{j}_g^+ = \left[ \left( \mathbf{j}_g^{+0} \right)^T \quad \left( \mathbf{j}_g^{+1} \right)^T \right]^T \quad (18)$$

where 0 and 1 denote the flat and non-flat surface moments respectively. Correspondingly, the WG iteration formulas can also be partitioned

$$\begin{bmatrix} \mathbf{j}_g^{+0} \\ \mathbf{j}_g^{+1} \end{bmatrix} = \begin{bmatrix} \mathbf{R}_g^{00} & \mathbf{R}_g^{01} \\ \mathbf{R}_g^{10} & \mathbf{R}_g^{11} \end{bmatrix} \begin{bmatrix} \boldsymbol{\Pi} \otimes \mathbf{I}_I \mathbf{j}_g^{+0} \\ \boldsymbol{\Pi} \otimes \mathbf{I}_K \mathbf{j}_g^{+1} \end{bmatrix} + \begin{bmatrix} \mathbf{B}_g^0 \\ \mathbf{B}_g^1 \end{bmatrix} \mathbf{s}_g \quad (19)$$

As in VARIANT, the WG iteration can be done only for the flat-moment system with non-flat ones fixed

$$\mathbf{j}_g^{+0} = \left[ \mathbf{R}_g^{00} \quad \mathbf{R}_g^{01} \right] \begin{bmatrix} \boldsymbol{\Pi} \otimes \mathbf{I}_I \mathbf{j}_g^{+0} \\ \boldsymbol{\Pi} \otimes \mathbf{I}_K \mathbf{j}_g^{+1} \end{bmatrix} + \mathbf{B}_g^0 \mathbf{s}_g \quad (20)$$

Once the flat-moment system converged, a full sweep can be carried out to update the all of the moments including the non-flat ones. The VNM iteration process is shown in Fig. 2.

By comparing the Eqs. (19) and (20), it can be found that the PM technique is designed to save numbers of updates on the non-flat partial current moments by requiring a number of more updates on the flat ones.

### 2.3. The Partitioned-Matrix acceleration for Fission-Source iteration

Due to the fact that the PM acceleration for WG iteration reduces computing times by smaller percentages than when used in higher order transport calculations, we extend the PM technique to the FS iteration in this paper.

Partitioning the surface partial current and the volume flux vectors:

$$\mathbf{j}_g^+ = \begin{bmatrix} (\mathbf{j}_g^{+\alpha})^\top & (\mathbf{j}_g^{+\beta})^\top \end{bmatrix}^\top \quad (21)$$

$$\boldsymbol{\varphi}_g = \begin{bmatrix} (\boldsymbol{\varphi}_g^l)^\top & (\boldsymbol{\varphi}_g^h)^\top \end{bmatrix}^\top \quad (22)$$

where  $\alpha$  and  $\beta$  denote the low ( $K1$ ) and high-order ( $K2$ ) surface moments, and  $l$  and  $h$  denote the low ( $I1$ ) and high-order ( $I2$ ) volume moments. Correspondingly, the iteration formulas can be partitioned

$$\begin{bmatrix} \mathbf{j}_g^{+\alpha} \\ \mathbf{j}_g^{+\beta} \end{bmatrix} = \begin{bmatrix} \mathbf{R}_g^{\alpha\alpha} & \mathbf{R}_g^{\alpha\beta} \\ \mathbf{R}_g^{\beta\alpha} & \mathbf{R}_g^{\beta\beta} \end{bmatrix} \begin{bmatrix} \Pi \otimes \mathbf{I}_{K1} \mathbf{j}_g^{+\alpha} \\ \Pi \otimes \mathbf{I}_{K2} \mathbf{j}_g^{+\beta} \end{bmatrix} + \begin{bmatrix} \mathbf{B}_g^\alpha \\ \mathbf{B}_g^\beta \end{bmatrix} \mathbf{s}_g \quad (23)$$

$$\begin{bmatrix} \boldsymbol{\varphi}_g^l \\ \boldsymbol{\varphi}_g^h \end{bmatrix} = \begin{bmatrix} \mathbf{H}_g^l \\ \mathbf{H}_g^h \end{bmatrix} \mathbf{s}_g - \begin{bmatrix} \mathbf{C}_g^{l\alpha} & \mathbf{C}_g^{l\beta} \\ \mathbf{C}_g^{h\alpha} & \mathbf{C}_g^{h\beta} \end{bmatrix} \begin{bmatrix} (\mathbf{I}_{N \cdot N_s} - \Pi) \otimes \mathbf{I}_{K1} \mathbf{j}_g^{+\alpha} \\ (\mathbf{I}_{N \cdot N_s} - \Pi) \otimes \mathbf{I}_{K2} \mathbf{j}_g^{+\beta} \end{bmatrix} \quad (24)$$

Before each full-order sweeping, a number of low-order sweeping is carried out with high-order moments fixed.

$k_{(0)} = 1.0, \quad \boldsymbol{\varphi}_{(0)} = 1, \quad \mathbf{j}_{(0)} = 0; \quad \hat{\mathbf{f}}_{(0)} = \mathbf{F} \otimes \mathbf{I}_l \boldsymbol{\varphi}_{(0)};$   
 FS iteration: Do  $n=1, \dots, N_{\max}$   
 $\mathbf{f}_{(n)} = (1/k_{(n-1)}) \hat{\mathbf{f}}_{(n-1)}$   
 MG iteration: Do  $m=1, \dots, M_{\max}$   
 EG sweeping: Do  $g=1, \dots, G$   
 $\mathbf{s}_g = \sum_{D,g} \otimes \mathbf{I}_l \boldsymbol{\varphi}^{\text{New}} + \sum_{U,g} \otimes \mathbf{I}_l \boldsymbol{\varphi}^{\text{Old}} + \mathbf{f}_g$   
 $\mathbf{q}_g = \mathbf{B}_g \mathbf{s}_g$   
 $\tilde{\mathbf{q}}_g = \mathbf{q}_g + \mathbf{R}_g^{01} \Pi \otimes \mathbf{I}_{K-1} \mathbf{j}_g^{+1}$   
 WG iteration: Do  $i=1, \dots, I_g^{\max}$   
 $\mathbf{j}_g^{+0(i)} = \mathbf{R}_g^{00} \Pi \otimes \mathbf{I}_1 \mathbf{j}_g^{+0(i-1)} + \tilde{\mathbf{q}}_g$   
 If  $\mathbf{j}_g^+$  converged, EXIT  
 End Do WG iteration  
 $\mathbf{j}_g^+ \leftarrow \mathbf{R}_g \Pi \otimes \mathbf{I}_K \mathbf{j}_g^+ + \mathbf{q}_g$   
 $\boldsymbol{\varphi}_g^{\text{New}} = \mathbf{H}_g \mathbf{s}_g - \mathbf{C}_g (\mathbf{I}_j - \Pi \otimes \mathbf{I}_K) \mathbf{j}_g^+$   
 End Do EG sweeping  
 If  $\boldsymbol{\varphi}$  converged, EXIT  
 End Do MG iteration  
 $\hat{\mathbf{f}}_{(n)} = \mathbf{F} \otimes \mathbf{I}_l \boldsymbol{\varphi}_{(n)}, \quad k_{(n)} = k_{(n-1)} \frac{\|\hat{\mathbf{f}}_{(n)}\|_1}{\|\hat{\mathbf{f}}_{(n-1)}\|_1}.$   
 If  $k$  and  $\mathbf{f}$  converged, EXIT  
 End Do FS iteration

Fig. 2. The VNM iteration process with partitioned-matrix acceleration for WG iteration.

$$\mathbf{j}_g^{+\alpha} = \begin{bmatrix} \mathbf{R}_g^{\alpha\alpha} & \mathbf{R}_g^{\alpha\beta} \\ \mathbf{R}_g^{\beta\alpha} & \mathbf{R}_g^{\beta\beta} \end{bmatrix} \begin{bmatrix} \Pi \otimes \mathbf{I}_{K1} \mathbf{j}_g^{+\alpha} \\ \Pi \otimes \mathbf{I}_{K2} \mathbf{j}_g^{+\beta} \end{bmatrix} + \mathbf{B}_g^\alpha \mathbf{s}_g \quad (25)$$

$$\boldsymbol{\varphi}_g^l = \mathbf{H}_g^l \mathbf{s}_g - \begin{bmatrix} \mathbf{C}_g^{l\alpha} & \mathbf{C}_g^{l\beta} \\ \mathbf{C}_g^{h\alpha} & \mathbf{C}_g^{h\beta} \end{bmatrix} \begin{bmatrix} (\mathbf{I}_{N \cdot N_s} - \Pi) \otimes \mathbf{I}_{K1} \mathbf{j}_g^{+\alpha} \\ (\mathbf{I}_{N \cdot N_s} - \Pi) \otimes \mathbf{I}_{K2} \mathbf{j}_g^{+\beta} \end{bmatrix} \quad (26)$$

By comparing the Eqs. (23) and (24) with Eqs. (25) and (26), it can be found that the PM technique for FS iteration is designed to save numbers of updates on the high-order currents and flux moments by requiring a number of more updates on low-order currents and flux moments.

The VNM iteration process is shown in Fig. 3. It can be found that the total computing effort in FLOP is mainly contributed by four steps: (1) the source construction or the applications of the scattering and fission matrices; (2) the nodal response or the applications of the response matrices  $\mathbf{B}, \mathbf{R}, \mathbf{H}$  and  $\mathbf{C}$ ; (3) the specification of nodal incoming partial current if discontinuity factors show up; (4) iterative error estimations.

### 3. Numerical results

Based on the formulations of the Variational Nodal Method, a code named VIOLET has been developed in Xi'an Jiaotong University for Pressurized Water Reactor core neutron-diffusion calculation. And the PM technique has been implemented to accelerate the

$k_{(0)} = 1.0, \quad \boldsymbol{\varphi}_{(0)} = 1, \quad \mathbf{j}_{(0)} = 0; \quad \hat{\mathbf{f}}_{(0)} = \mathbf{F} \otimes \mathbf{I}_l \boldsymbol{\varphi}_{(0)};$   
 FS iteration: Do  $n=1, \dots, N_{\max}$   
 $\mathbf{f}_{(n)} = (1/k_{(n-1)}) \hat{\mathbf{f}}_{(n-1)}$   
 MG iteration: Do  $m=1, \dots, M_{\max}$   
 EG sweeping: Do  $g=1, \dots, G$   
 $\mathbf{s}_g = \sum_{D,g} \otimes \mathbf{I}_l \boldsymbol{\varphi}^{\text{New}} + \sum_{U,g} \otimes \mathbf{I}_l \boldsymbol{\varphi}^{\text{Old}} + \mathbf{f}_g$   
 If the  $n$ 'th FS iteration is Partitioned, then  
 $\mathbf{q}_g^\alpha = \mathbf{R}_g^{\alpha\beta} \Pi \otimes \mathbf{I}_{K2} \mathbf{j}_g^{+\beta} + \mathbf{B}_g^\alpha \mathbf{s}_g$   
 WG iteration: Do  $i=1, \dots, I_g^{\max}$   
 $\mathbf{j}_g^{+\alpha(i)} = \mathbf{R}_g^{\alpha\alpha} \Pi \otimes \mathbf{I}_{K1} \mathbf{j}_g^{+\alpha(i-1)} + \mathbf{q}_g^\alpha$   
 If  $\mathbf{j}_g^{+\alpha}$  converged, EXIT  
 End Do WG iteration  
 $\boldsymbol{\varphi}_g^{l,\text{New}} = \mathbf{H}_g^l \mathbf{s}_g - \begin{bmatrix} \mathbf{C}_g^{l\alpha} & \mathbf{C}_g^{l\beta} \\ \mathbf{C}_g^{h\alpha} & \mathbf{C}_g^{h\beta} \end{bmatrix} \begin{bmatrix} (\mathbf{I}_{N \cdot N_s} - \Pi) \otimes \mathbf{I}_{K1} \mathbf{j}_g^{+\alpha} \\ (\mathbf{I}_{N \cdot N_s} - \Pi) \otimes \mathbf{I}_{K2} \mathbf{j}_g^{+\beta} \end{bmatrix}$   
 Else  
 $\mathbf{q}_g = \mathbf{B}_g \mathbf{s}_g$   
 WG iteration: Do  $i=1, \dots, I_g^{\max}$   
 $\mathbf{j}_g^{+(i)} = \mathbf{R}_g \Pi \otimes \mathbf{I}_K \mathbf{j}_g^{+(i-1)} + \mathbf{q}_g$   
 If  $\mathbf{j}_g^+$  converged, EXIT  
 End Do WG iteration  
 $\boldsymbol{\varphi}_g^{\text{New}} = \mathbf{H}_g \mathbf{s}_g - \mathbf{C}_g (\mathbf{I}_j - \Pi \otimes \mathbf{I}_K) \mathbf{j}_g^+$   
 End If  
 End Do EG sweeping  
 If  $\boldsymbol{\varphi}$  converged, EXIT  
 End Do MG iteration  
 $\hat{\mathbf{f}}_{(n)} = \mathbf{F} \otimes \mathbf{I}_l \boldsymbol{\varphi}_{(n)}, \quad k_{(n)} = k_{(n-1)} \frac{\|\hat{\mathbf{f}}_{(n)}\|_1}{\|\hat{\mathbf{f}}_{(n-1)}\|_1}.$   
 If  $k$  and  $\mathbf{f}$  converged, EXIT  
 End Do FS iteration

Fig. 3. The VNM iteration process with partitioned-matrix acceleration for FS iteration.

FS iteration. Neutron diffusion calculation usually is employed for assembly or quarter assembly homogenized reactor core calculation. During the homogenization process, the neutron leakage rates during spatial homogenization can be preserved by using Generalized Equivalence Theory with discontinuity factor (Smith, 1986, 1980) or other homogenization techniques without discontinuity factor, such as superhomogenization (Hébert, 2009). Considering the fact that the application of discontinuity factor slows the nodal iteration convergence (Zika and Downar, 1993), two typical test problems without and without discontinuity factor respectively have been chosen to evaluate and analyze the code and the algorithms. During these tests for PM technique, all other acceleration techniques such as the multi-level iteration optimization (Li et al., 2013) in VIOLET are turned off. These calculations were performed using a 32 bit Intel® Core™ i7-2600 CPU @3.40 GHz with Windows 7 operating system and 3 GB memory.

3.1. PWR problem without discontinuity factor

As shown in Fig. 4, the first test problem is a quarter core problem representing a typical PWR operating state. There are 5 types of fuel assemblies named A-E, containing 5 different materials tagged by numbers 1 to 5 as listed in Table 1. Each type of assembly has its own axial composition as shown in Fig. 4. There are partially and fully inserted control rods in assemblies E and C respectively. Assembly D is the reflector. The mesh sizes are the same as the assembly size in radial direction, and 20 cm each in the axial direction. Totally, there are 1311 spatial nodes with 6 surfaces per node.

The volumetric flux is represented by a 5th order polynomial in radial and 7th order polynomial axially, while the partial current on each interface is represented by a 2nd order polynomial. This leads to 58 degrees of freedoms (DOFs) per node, and 6 DOFs for each node surface. The convergence criteria for  $k_{eff}$  and fission source were set as  $e_k = 1.0 \times 10^{-5}$  and  $e_f = 1.0 \times 10^{-4}$  respectively, with the maximum number of FS iterations set to be 500. Due to the absence of up-scattering, there is no MG iteration. For the WG iteration of each energy group, a maximum iteration number  $I_{gmax} = 100$ , an AET  $\epsilon_{WG} = 1.0 \times 10^{-12}$  and a RET  $e_{WG} = 1.0 \times 10^{-3}$  were employed for the partial current update. It is worth to point out that the numerical results before and after acceleration are the same with the convergence criteria, which means the difference between them are less than  $1.0 \times 10^{-4}$ .

For this problem, computing effort in FLOP for the full-order response matrices **B**, **R**, **H** and **C** are respectively 2088, 1296, 3364 and 2088. After 244 FS iterations with 9044 WG iterations, the results converged to the right answer. For the PM acceleration, the

**Table 1**  
Cross sections for the PWR problem without discontinuity factor.

Material	g	D <sup>g</sup> /cm	$\Sigma_a^g/cm^{-1}$	$\nu \Sigma_f^g/cm^{-1}$	$\Sigma_a^{21}/cm^{-1}$
1	1	1.5	0.01	0	0.02
	2	0.4	0.08	0.135	
2	1	1.5	0.01	0	0.02
	2	0.4	0.085	0.135	
3	1	1.5	0.01	0	0.02
	2	0.4	0.13	0.135	
4	1	2.0	0	0	0.04
	2	0.3	0.01	0	
5	1	2.0	0	0	0.04
	2	0.3	0.055	0	

number of low-order current moments K1 is 1 (flat), while first 4 (linear in three dimensional spaces) volumetric flux moments are considered as the low-order ones. The number of low-order FS iterations before each full-order one is determined by the reduction of  $k_{eff}$  error. The low-order improvement is taken as achieved once the relative error of  $k_{eff}$  ( $e_k$ ) is reduced by 50%. In this case, it turned out that only 20 full-order FS iterations (containing 802 full-order WG iterations) together with 272 low-order ones (containing 8553 low-order WG iterations) are required to reach the same results.

As listed in Table 2, without the PM acceleration, 35-second CPU time is needed by the entire iteration process to complete  $21 \times 10^9$  FLOP. Among those FLOP, there are  $16 \times 10^9$  FLOP (about 76%) required by the WG iteration. In contrast, only 8-second CPU time would be needed to carry out  $3 \times 10^9$  FLOP when PM technique is applied. The CPU time for full-order iteration is reduced to about 4 s while introducing about 4 s for extra low-order iterations. Fig. 5 shows the convergences of  $k_{eff}$  and fission source with and without employing of the PM technique. It can be found that the errors would rebound after each full-order sweep, but the low-order sweeps reduces it again quickly. And for the first full-order sweeps, less number of low-order sweeps would be required since the error of source distribution is large. Once the error of source distributing becomes small, more low-order iterations are going to be required to reduce the error of  $k_{eff}$  by 50%. In addition, non-monotonic convergence is observed in the accelerated case, which is usual for coarse mesh accelerations.

3.2. PWR problem with discontinuity factor

As shown in Fig. 6, the second test problem is also a quarter core problem referring to a typical PWR operating state. Comparing to the first problem, there are several facts making it much more

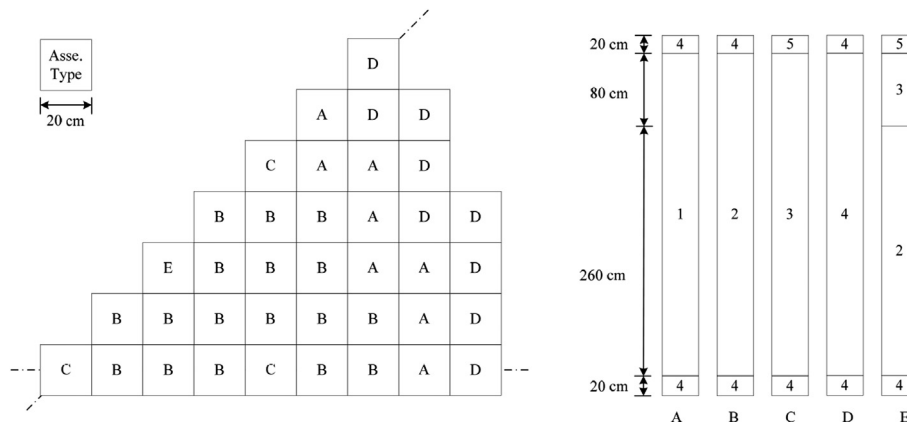


**Fig. 4.** The configuration for the PWR problem without discontinuity factor.

**Table 2**  
Computing efforts for the PWR problem without discontinuity factor.

		Total	Full-order FS excluding WG	Full-order WG	Low-order FS excluding WG	Low-order WG
Without PM	Time (s)	34.7	8.9	25.8	–	–
	FLOP ( $10^9$ )	20.7	4.9	15.8	–	–
With PM	Time (s)	8.3	1.5	2.3	1.1	3.4
	FLOP ( $10^9$ )	2.6	0.4	1.4	0.3	0.5

realistic. Firstly, there are three batches of full assemblies including new ones and the ones experienced 1 and 2 cycles already. Secondly, there are numbers of burnable poisons (Gd) rod in these assemblies. The numbers Gd rods per assembly are among 0, 8, 20 and 24. Thirdly, all control rods are out of the core, but the boron concentration is 1830 ppm (the corresponding critical boron concentration is 1953 ppm). Fourthly, each assembly is divided into 4 nodes in radial direction and 20 cm per node in axial. Totally, there are 3978 spatial nodes with 6 surfaces per node. The cross sections are provided by using the CASMO-4 (University release) (Studsvik Scandpower, 2009).

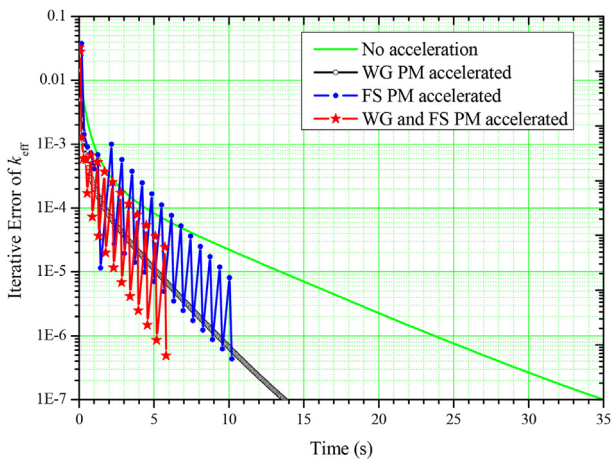


**Fig. 5.** Fission-Source iteration processes of the PWR problem without discontinuity factor.

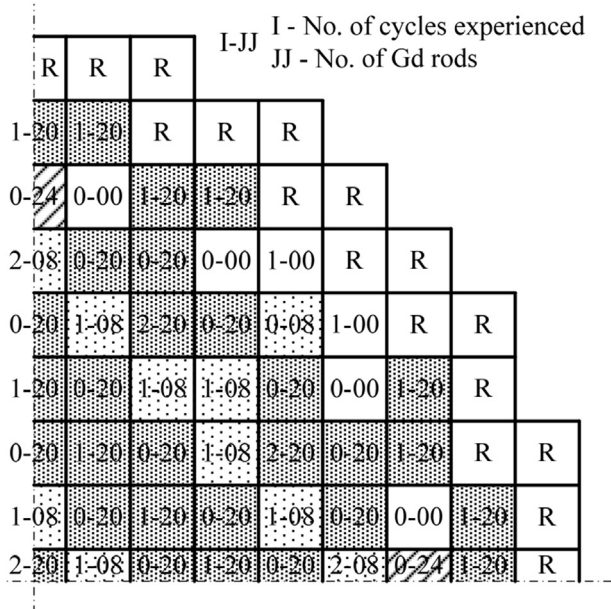


**Fig. 6.** The configuration for the PWR problem with discontinuity factor.

The volumetric flux is represented by a 7th order polynomial radially 5th order polynomial axially, while the surface partial current is represented as a 3rd order polynomial. It leads to 71 DOFs per node and 10 DOFs per nodal surface. The convergence criteria are the same with the first problem. Correspondingly, computing effort in FLOP for the full-order response matrices **B**, **R**, **H** and **C** are respectively 4260, 3600, 5041 and 4260. After 386 FS iterations with 11,177 WG iterations, the results converged to the right answer. For the PM acceleration, the number low-order current moment  $K_1$  is 1 (flat), while 1 (flat) volumetric flux moments is considered as the low-order ones. The number of low-order FS iterations before each full-order one is determined by the reduction of  $k_{eff}$  error. The low-order improvement is achieved once the relative error of  $k_{eff}$  ( $e_k$ ) is reduced by 50%. In this case, only 37 full-order FS iterations (containing 2156 full-order WG iterations) together with 309 low-order ones (containing 8311 low-order WG iterations) are required to reach the same results (the difference between the numerical results before and after acceleration is less than  $1.0 \times 10^{-4}$ ).

As in Table 3, the total computational efforts required by the original VNM iteration is  $210 \times 10^9$  FLOP, and correspondingly 442 s of CPU time. Again, about 76% effort was spent on the WG iterations. With the PM acceleration, the total computing time is reduced to 120 s to complete  $40 \times 10^9$  FLOP. The computing effort in full-order FS iteration was reduced to  $37 \times 10^9$  FLOP while  $3 \times 10^9$  extra FLOP are added in the low-order FS iterations. The FS iteration is shown in Fig. 7, indicates that the same acceleration performance of the PM technique can be achieved for the PWR core when the discontinuity factors are presented.

**4. Conclusion and discussion**

The legacy Partitioned-Matrix (PM) technique traditionally developed for the within-group (WG) iteration acceleration is now extended to accelerate the Fission-Source (FS) iteration of the Variational Nodal Method (VNM) for PWR core neutron-diffusion calculation. Based on our new VNM code VIOLET, numerical test were carried out for two typical PWR problems with and without using discontinuity factors. By analyzing both the computational effort in terms of FLOP (FLoating-point OPeration) and the computing time, it has been demonstrated that the PM technique can provide an acceleration ratio of about 4 for the test problems. By extending the PM technique from the WG iteration to the FS iteration, the neutron-diffusion calculation can be accelerated very effectively with almost no extra storage or implementation cost to the existing computer code. The PM technique roots in the orthogonality of the basis functions. Considering the fact that the PM technique performs very well in accelerating the WG iteration for the VNM neutron-transport calculation, its extension from WG iteration to FS iteration is also expected to work well for the VNM neutron-transport calculation.

Based on the idea of macroscopic acceleration, the PM technique is employed to accelerate the FS iteration of the VNM. The general term macroscopic acceleration used here represents all the acceleration techniques that uses coarse-mesh or low-order expansion methods in space, angle or energy to accelerate the original fine-

**Table 3**  
Computing efforts for the PWR problem with discontinuity factor.

		Total	Full-order FS excluding WG	Full-order WG	Low-order FS excluding WG	Low-order WG
Without PM	Time (s)	442.2	103.2	339.0	–	–
	FLOP ( $10^9$ )	210.8	42.7	168.1	–	–
With PM	Time (s)	119.7	17.8	64.8	11.5	25.6
	FLOP ( $10^9$ )	40.0	4.1	32.4	1.7	1.8

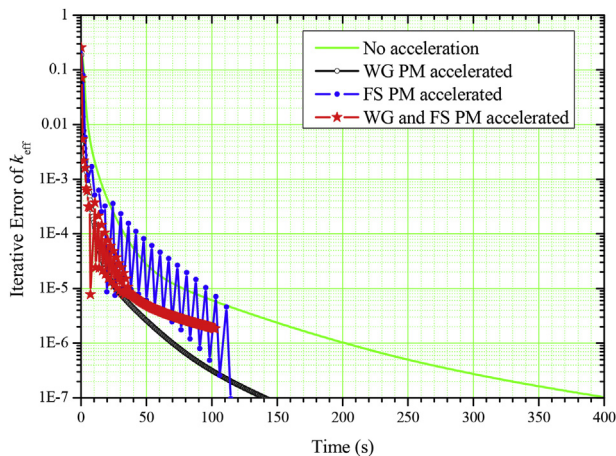


**Fig. 7.** Fission-Source iteration processes of the PWR problem with discontinuity factor.

mesh or high-order methods, such as the Coarse Mesh Rebalance (CMR) (Lewis and Miller, 1984; Xie and Deng, 2005), Coarse Mesh Finite Differencing (CMFD) (Smith and Rhodes, 2002; Joo et al., 2002; Zhong et al., 2008), Diffusion Synthetic Acceleration (DSA) (Koph, 1963; Larsen, 1982; McCoy and Larsen, 1982; Azmy et al., 1985), Non-Linear Iteration technique (NLI) (Smith, 1983; Liao, 2002) and other coarse mesh acceleration methods (Li, 2013; Tatsumi and Yamamoto, 2003). There are two features in these methods. Firstly, they use an efficient coarse-mesh calculation to accelerate a fine-mesh calculation which is expensive in both computing efforts and storage. Secondly, since the coarse-mesh method is not as accurate as the fine-mesh calculation, the coarse-mesh calculation has to be corrected by the corresponding fine-mesh iterative result. There are different ways to implement the correction. One can correct the diffusion coefficient as in CMR and DSA, or add a new term as in CMFD, or define a discontinuity factor as in EFEN method (Li, 2013). The philosophy behind these CMA methods is to catch the source profile during iteration as early as possible. From this point of view, the PM technique is one of those CMA methods. It uses the low-order spatial expansion moments corrected by adding the high-order moments to balance the source distribution quickly. By extending the PM technique from the WG iteration to the FS iteration, the neutron-diffusion calculation of the VNM can be accelerated very effectively with almost no extra storage and implementation costs to the existing code.

## Acknowledgments

This work is supported by the National Natural Science Foundation of China (No. 11305123).

## References

Azmy, Y.Y., Morning, J.J., April 9–11, 1985. Diffusion synthetic acceleration of the multi-dimensional discrete nodal transport method. In: Proc. of International Topical Meeting on Advances in Nuclear Engineering Computational Methods. Knoxville, TN USA.

- Carrico, C.B., Lewis, E.E., Palmiotti, G., 1992. Three-dimensional variational nodal transport methods for Cartesian, triangular and hexagonal criticality calculations. Nucl. Sci. Eng. 111, 168–179.
- Doriath, J.Y., Ruggieri, J.M., Buzzi, G., et al., 1994. Reactor analysis using the Variational Nodal Method implemented in the ERANOS system. In: PHYSOR1994, Knoxville, TN USA, April 11–15, vol. III, pp. 464–471.
- Hébert, A., 2009. Applied Reactor Physics. Presses Internationales Polytechnique, Montréal.
- Joo, H.G., Cho, J.Y., Kim, H.Y., et al., 2002. Dynamic implementation of the equivalence theory in the heterogeneous whole core transport calculation. In: Proceeding of PHYSOR 2002, Seoul.
- Koph, H.J., 1963. Synthetic method solution of the transport equation. Nucl. Sci. Eng. 17 (1), 65–74.
- Larsen, E.W., 1982. Unconditionally stable diffusion-synthetic acceleration methods for the slab geometry discrete ordinate equation part I: theory. Nucl. Sci. Eng. 82 (1), 47–63.
- Lawrence, R.D., 1986. Progress in nodal methods for the solution of the neutron diffusion and transport equations. Prog. Nucl. Energy 17, 271–301.
- Lewis, E.E., Miller Jr., W.F., 1984. Computational Methods of Neutron Transport. John Wiley & Sons, Inc, New York & United States.
- Lewis, E.E., Li, Y., Smith, M.A., et al., 2013. Preconditioned Krylov solution of response matrix equations. Nucl. Sci. Eng. 173 (3), 222–232.
- Li, Y., 2013. Advanced Reactor Core Neutronics Computational Algorithms Based on the Variational Nodal and Nodal SP<sub>3</sub> Methods (in Chinese). Xi'an Jiaotong University, Xi'an, China.
- Li, Y., Lewis, E.E., Smith, M.A., 2012. Comparison of two  $p$  preconditioned GMRES algorithms for variational nodal multi-group system. Trans. Am. Nucl. Soc. 106, 398–400.
- Li, Y., Lewis, E.E., Smith, M.A., 2013. Multi-level iteration optimization for the Variational Nodal Method with multi-group GMRES algorithm. Trans. Am. Nucl. Soc. 108, 435–438.
- Li, Y., Wang, Y., Wu, H., et al., 2014. Heterogeneous Variational Nodal Method with continuous cross section distribution in space. Trans. Am. Nucl. Soc. 111, 727–729.
- Li, Y., Lewis, E.E., Smith, M.A., et al., 2015. Preconditioned multi-group GMRES algorithms for the Variational Nodal Method. Nucl. Sci. Eng. 179 (1), 42–58.
- Liao, C., 2002. Study on Numerical Method for Three Dimensional Nodal Space-time Neutron Kinetic Equations and Coupled Neutronic/Thermal-hydraulic Core Transient Analysis (in Chinese). Xi'an Jiaotong University, Xi'an, China.
- McCoy, D.R., Larsen, E.W., 1982. Unconditionally stable diffusion-synthetic acceleration methods for the slab geometry discrete ordinate equation part II: numerical results. Nucl. Sci. Eng. 82 (1), 64–70.
- Palmiotti, G., Lewis, E.E., Carrico, C.B., 1995. VARIANT: Variational Anisotropic Nodal Transport for Multidimensional Cartesian and Hexagonal Geometry Calculation. ANL-95/40. Argonne National Laboratory.
- Palmiotti, G., Smith, M.A., Rabiti, C., Leclere, M., Kaushik, D., Siegel, A., Smith, B., Lewis, E.E., 2007. UNIC: ultimate neutronic investigation code. In: Proc. M&C 2007, Monterey CA, USA, April 15–19.
- Saad, Y., 2003. Iterative Methods for Sparse Linear Systems, second ed. SIAM, Philadelphia.
- Saad, Y., Schultz, M.H., 1986. GMRES: a generalized minimal residual algorithm for solving nonsymmetric linear systems. SIAM J. Sci. Stat. Comput. 7, 856–869.
- Smith, K.S., 1980. Spatial Homogenization Methods for Light Water Reactors (PhD thesis). MIT.
- Smith, K.S., 1983. Nodal method strategy reduction by nonlinear iteration. Trans. Am. Nucl. Soc. 44, 265.
- Smith, K.S., 1986. Assembly homogenization techniques for light water reactor analysis. Prog. Nucl. Energy 17, 303.
- Smith, K.S., Rhodes, J.D., 2002. Full-core, 2-D, LWR core calculation with CASMO-4E. In: Proceeding of PHYSOR 2002, Seoul, Korea.
- Smith, M.A., Tsoufanidis, N., Lewis, E.E., et al., 2003. A finite subelement generalization of the Variational Nodal Method. Nucl. Sci. Eng. 144 (1), 36–46.
- Studsvik Scandpower, 2009. CASMO-4, a Fuel Assembly Burnup Program, User's Manual – University Release. SSP-09/443-U Rev 0.
- Tatsumi, M., Yamamoto, A., 2003. Advanced PWR core calculation based on multi-group nodal-transport method in three-dimensional pin-by-pin geometry. J. Nucl. Sci. Tech. 40, 376.
- Topfel, B.J., March 1983. The Fuel Cycle Analysis Capability REBUS-3. Argonne-83-2 Argonne National Laboratory.
- Wagner, M.R., 1989. Three-dimensional nodal transport methods for hexagonal-z geometry. Nucl. Sci. Eng. 103, 377–391.
- Wang, Y., Rabiti, C., Palmiotti, G., 2011. Krylov solvers preconditioned with the low-order red-black algorithm for the Pn hybrid FEM for the INSTANT code. In: M&C

- 2011, Rio de Janeiro, RJ, Brazil, May 8–12.
- Wang, Y., Wu, H., Li, Y., et al., Heterogeneous Variational Nodal Method in one dimensional slab geometry. (Submitted to Nucl. Eng. Des.).
- Xie, Z., Deng, L., 2005. Numerical Calculation Method of Neutron-transport Theory. Northwestern Polytechnical University Press, Xi'an, China.
- Zhong, Z., Downar, T.J., Xu, Y., et al., 2008. Implementation of two-level coarse-mesh finite difference acceleration in an arbitrary geometry, two-dimensional discrete ordinates transport method. Nucl. Sci. Eng. 158, 289–298.
- Zika, M.R., Downar, T.J., 1993. Numerical divergence effects of equivalence theory in the Nodal Expansion Method. Nucl. Sci. Eng. 115, 219–232.